Analytica Chimica Acta 1325 (2024) 343095

Contents lists available at ScienceDirect

Analytica Chimica Acta

journal homepage: www.elsevier.com/locate/aca

New screen-printed electrodes for Raman spectroelectrochemistry. Determination of *p*-aminosalicylic acid

Luis Romay [a], Pello Nuñez-Marinero [b], Juan V. Perales-Rondon [a,c], Aranzazu Heras [a], F. Javier del Campo [b,d,**], Alvaro Colina [a,*]

[a] Department of Chemistry, Universidad de Burgos, Pza. Misael Bañuelos s/n, E-09001, Burgos, Spain
[b] BCMaterials, Basque Center for Materials, Applications and Nanostructures. UPV/EHU Parque Científico, E-48940, Leioa, Bizkaia, Spain
[c] Hydrogen and Power-to-X Department, Iberian Centre for Research in Energy Storage, Polígono 13, Parcela 31, «El Cuartillo», E-10004, Cáceres, Spain
[d] IKERBASQUE, Fundación Vasca para la Ciencia, E-48009, Bilbao, Spain

HIGHLIGHTS

- New screen-printed electrodes for EC-SOERS analysis.
- Three electrode system based on silver.
- Raman enhancement depends on the type of silver ink.
- Determination of 4-aminosalicylic acid in complex matrices.

GRAPHICAL ABSTRACT

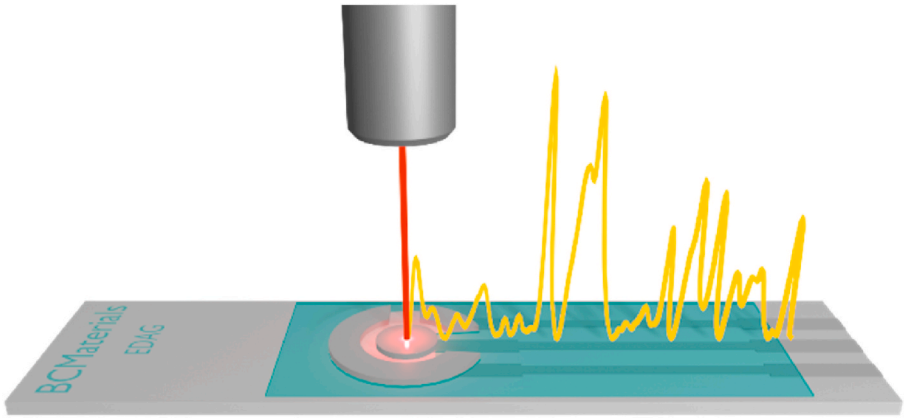

ARTICLE INFO

Handling Editor: Dr Jing-Juan Xu

Keywords:
Screen-printed electrodes
Raman spectroelectrochemistry
Electrochemistry
EC-SERS
EC-SOERS
4-Aminosalicylic acid

ABSTRACT

Background: The availability of new surface enhanced Raman scattering (SERS) substrates is essential to develop quantitative analytical methods. Electrochemistry is an easy, fast and reproducible methodology to prepare SERS substrates on screen-printed electrodes (SPEs).
Results: This work proposes new SPEs based on a three-electrode system all made of silver. Using the same ink for the whole electrode system facilitates the fabrication process, reduces production costs, and leads to excellent analytical performance. The results showed that Raman enhancement depends strongly on the type of silver ink. To demonstrate the capabilities of the new electrodes developed, 4-aminosalicylic acid was determined in complex matrices and in the presence of strong interfering compounds such as salicylic acid and acetylsalicylic acid. The proposed analytical method is based on the electrochemical surface oxidation enhanced Raman scattering (EC-SOERS) strategy. AgCl nanocrystals are generated on the working electrode surface, which amplify the

* Corresponding author.
** Corresponding author.
E-mail addresses: javier.delcampo@bcmaterials.net (F.J. del Campo), acolina@ubu.es (A. Colina).

https://doi.org/10.1016/j.aca.2024.343095
Received 8 May 2024; Received in revised form 2 July 2024; Accepted 11 August 2024
Available online 12 August 2024

Raman signal of 4-aminosalicylic acid. Good figures of merit were obtained both in the absence and in the presence of the interfering compounds, achieving a correct estimation of a 4-aminosalicylic test sample in complex matrices.

Significance: The new SPEs have been demonstrated to be very sensitive and reproducible which, together to the high specificity of the Raman signal, makes this methodology very attractive for chemical analysis.

1. Introduction

Surface enhanced Raman scattering (SERS) is a plasmon-based phenomenon first observed by Martin Fleischman and co-workers in 1974 during the roughening of a silver electrode in the presence of pyridine [1]. This phenomenon enhances the Raman intensity of a target molecule by up to 8-10 orders of magnitude [2–4] when these molecules are adsorbed onto or close enough to a nanostructured substrate surface, usually a coinage metal [2–5]. Since its discovery, different substrates have been reported to enhance the Raman intensity, including not only metallic materials, but also semiconductors and hybrid materials [6–8]. In 2018, our research group reported for the first time the phenomenon known as electrochemical surface oxidation enhanced Raman scattering (EC-SOERS), a new SERS-based strategy taking place at the surface of semiconductor or dielectric materials [9]. In contrast to previously thought, the Raman signal was enhanced during the oxidation of a silver electrode in the presence of a low chloride concentration in an acidic medium. Since this discovery, several new materials have been reported to promote SOERS behaviour, opening new avenues for analytical applications [10–15].

SERS, and more recently SOERS, have become widely used in different fields of science, including electrochemistry, catalysis, biology, medicine, materials science, etc [16–20]. Both phenomena, based on Raman enhancement from the interaction between adsorbed molecules and the surface of certain nanostructures, have been demonstrated to have a high sensitivity but low reproducibility due to their enhancing nature [2–5]. Improving the reproducibility of SERS/SOERS measurements has been attempted over the years following different methodologies, the most common of which involve the production of more suitable substrates by physical or chemical means. In recent years, electrochemical substrates based on screen-printed electrodes (SPEs) have emerged as an attractive strategy. Their scalability and high reproducibility have led to new analytical methodologies [17,21,22]. In this regard, the use of time-resolved Raman spectroelectrochemistry (TR-Raman-SEC) emerges as an appealing technique when using SPEs, which helps to improve the reproducibility in the electrochemical preparation of SERS substrates [21]. Electrochemical methods allow the generation of SERS/SOERS substrates in a simple and reproducible experiment [17,22], while the Raman signal is continuously monitored, which is useful for qualitative and quantitative purposes [17,21,22].

All the studies relying on SPEs for the generation of SERS substrates have been performed using commercially available SPEs [12,17,23,24]. Although bulk Ag electrodes yield higher Raman signals, Ag SPEs are more reproducible and have also been successfully used for EC-SOERS. In addition, the nature of the silver electrode surface seems to be critical to obtain good analytical signals. Moreover, some SPEs need specific electrochemical pre-treatment before they can be effectively used in SOERS [12,13,15]. This work presents a novel and robust silver-based SPE with excellent properties for analytical chemistry. This is demonstrated through the determination of *p*-aminosalicylic acid (PAS) as a target molecule.

PAS, also known as 4-aminosalicylic acid, is an amino derivative of salicylic acid (SA). It plays a key role as an antibiotic in the treatment of tuberculosis, especially against active drug-resistant tuberculosis, where is used in combination with other anti-tuberculosis drugs [25]. Therefore, the development of methods for quantitative determination of PAS is of paramount importance. The literature covers several methodologies for the determination of this molecule, including colorimetric [26,27] and HPLC-based methods [28–30]. However, these methodologies suffer from exhaustive sample pre-treatment, which result in time-consuming and complex analysis.

In this work, a novel SPE has been developed for TR-Raman-SEC. The new SPEs were printed with silver ink only in order to reduce the cost of the manufacturing process. This new approach for SPEs fabrication, useful in quantitative Raman spectroelectrochemistry, consists of three electrodes, namely, a working electrode (WE), a pseudo-reference electrode (RE), and a counter electrode (CE), all of them based on Ag and printed on a mirror-polished alumina substrate. Compared to commercial SPEs, the all-silver SPEs presented here led to the preparation of very sensitive SERS substrates without the need of pre-treatment step. Finally, it was demonstrated that these new SPEs can be used in the quantitative determination of PAS in complex samples, illustrating the potential of these new SPEs for analytical applications.

2. Materials and methods

2.1. Chemicals and materials

p-Aminosalicylic acid (PAS, 98+ %, Sigma-Aldrich), acetylsalicylic acid (AA, 99 %, Sigma-Aldrich), salicylic acid (SA, 99 %, Sigma-Aldrich), perchloric acid ($HClO_4$, 60 %, reagent, Panreac) and potassium chloride (KCl, 99+ %, reagent, ACROS Organics) were used as received without further purification. Aqueous solutions were freshly prepared using ultrapure water (18.2 MΩ-cm resistivity at 25 °C, 2 ppb TOC, Milli-Q Direct 8, Millipore).

Aspirin® (BAYER), each capsule contains: 500 mg of AA and the following excipients: cellulose powder and corn starch.

Adiro® (BAYER), each capsule contains: 100 mg of AA and the following excipients: cellulose powder, corn starch, methacrylic acid copolymer type C, sodium dodecyl sulphate, polysorbate 80, talc and triethyl citrate.

2.2. Instrumentation

TR-Raman-SEC measurements were performed with a customized SPELEC RAMAN (Metrohm-DropSens). A laser source of 785 nm was used in all the experiments, with a laser power of 60.2 mW (192 Wcm^{-2}). The software used to acquire the spectroelectrochemical data was DropView SPELEC (Metrohm-DropSens). Different customized silver SPEs were used in all experiments. These SPEs consist of three Ag electrodes, namely, WE, RE, and CE, all of them printed on a single-side polished 96 % alumina ceramic substrates (Biotain, CN) using Loctite Electrodag 725S Ag ink (Tetrachim, FR).

2.3. Spectroelectrochemistry measurements

Cyclic voltammetry (CV) was selected as the electrochemical technique to perform the TR-Raman-SEC experiments. The vertex potentials were 0 V and +0.40 V, starting at 0.00 V in the anodic direction; the scan rate was 0.02 Vs^{-1} in all experiments. All potentials are referenced to a silver pseudo-RE. Unless otherwise stated, the acquisition time of the Raman spectra was 1 s throughout this work. All experiments were performed directly on the new silver SPEs, without any pre-treatment and/or modification. Experiments using commercial C013 Ag SPEs (Methrom-DropSens) were performed after a pre-treatment consisting on applying the same electrochemical protocol in a solution containing

0.1 M $HClO_4$ and 5 mM KCl in the absence of analyte. After conditioning of the commercial SPEs, the molecule detection protocol described above was carried out.

2.4. Scanning electron microscope images

SEM images were acquired using a Field-Emission Scanning Electron Microscope (FE-SEM), model GeminiSEM560 (Zeiss), applying an electron beam of 2 kV using an in-lens secondary electrons detector.

2.5. Sample preparation

All PAS solutions were diluted in 0.1 M $HClO_4$ and 5 mM KCl as electrolytic medium. To further test the interferent's effect, all PAS solutions were prepared containing different amounts of SA and AA as will be detailed below.

The Aspirin® (BAYER) sample was prepared as follows: 3 Aspirin® pills with a net weight of 1.80 g (1.50 g of AA content according to the package label) were diluted in water up to 2 L. This sample and a stock solution of PAS were diluted to a nominal concentration of 15 μM AA and a spiked concentration of 15 μM of PAS, resulting in test sample 1 (TS_A), being AA acting as interferent.

The Adiro® (BAYER) sample was prepared as follows: 12 Adiro® pills with a net weight of 1.64 g (1.2 g of AA content according to the package label) were diluted in water up to 2 L. This sample and a stock solution of PAS were diluted to a nominal concentration of 15 μM AA and a spiked concentration of 15 μM of PAS, resulting in test sample 2 (TS_B) being AA acting as interferent.

3. Results

3.1. Band identification

Before carrying out a TR-Raman-SEC experiment, the spectroscopic features of the three molecules studied were assessed. Raman spectra of the solid samples as well as the SOERS spectra during a SEC experiment were measured for PAS, which is the target molecule, and for SA and AA as interfering molecules in this study. The Raman spectra for samples in solid state were obtained measuring the pure chemical powder, Fig. 1A, while the SOERS spectra were obtained in solution, Fig. 1B, during a SEC experiment following the electrochemical protocol described in section 2.3.

The normal Raman and SOERS spectra of the three molecules are very similar since they belong to the same family, and share a common molecular structure. Despite that, PAS displays a higher SOERS spectrum, while AA shows the lowest SOERS spectrum among the 3 compounds, indicating a different cross-section for these molecules. In addition, small differences can be observed between the Raman spectrum of the solid and the SOERS spectrum of the same molecule. These small differences can be related to the interaction of the molecules in the aqueous medium and/or with the SOERS substrate. The band assignment of the PAS spectrum is listed in Table S1 [31].

3.2. TR-Raman-SEC experiments

As mentioned above, the generation of suitable SOERS substrates for reproducible Raman signal enhancement in low concentration solutions is exceptionally important. In this case, the SOERS substrate is generated *in-situ* by electrochemical oxidation of the silver electrode surface in the presence of 0.1 M $HClO_4$ and 5 mM KCl.

As Fig. 2A shows, the first anodic peak at +0.05 V corresponds to the oxidation of Ag^0 from the surface to form AgCl, which precipitates and deposits on the WE as nanocrystals [32]. Afterwards, from +0.25 V onwards and up to the vertex potential at +0.40 V, the massive oxidation peak of Ag^0 to free Ag^+ can be observed. Finally, in the backward scan, a cathodic peak at +0.30 V corresponds to the reduction of Ag^+ to

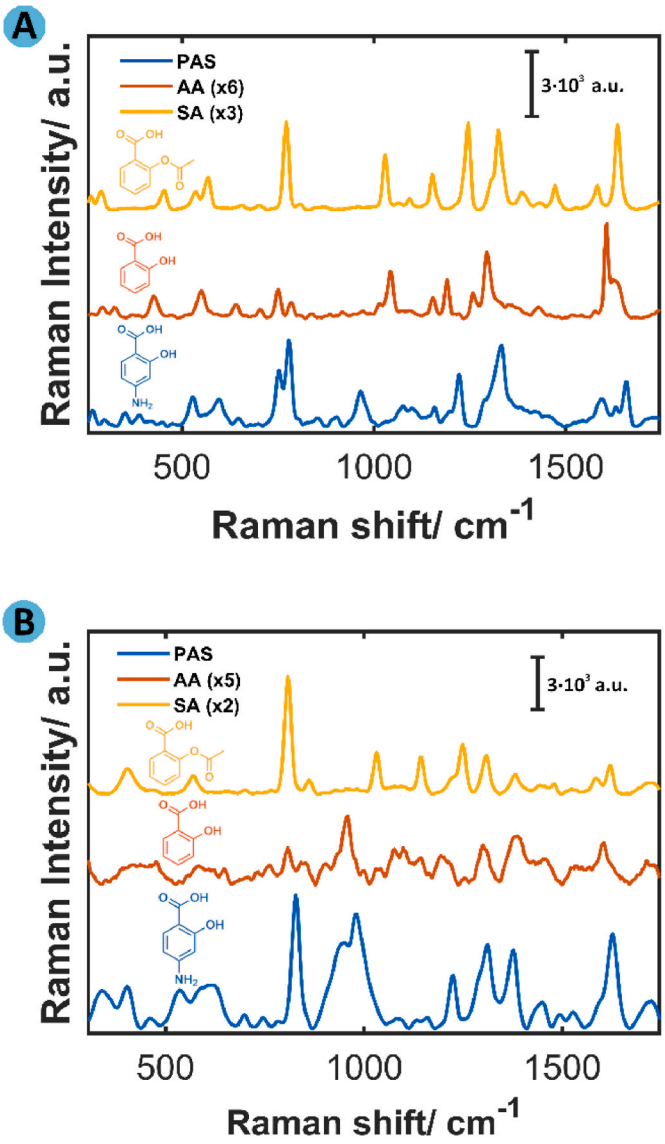

Fig. 1. (**A**) Raman spectra for PAS, AA and SA in solid state. (**B**) SOERS spectra for 1 mM PAS, 1 mM AA and 1 mM SA, all in the presence of 0.1 M $HClO_4$ and 5 mM KCl. The spectra included have been scaled as indicated in the figure to be similar in intensity for ease comparison. Molecular structure of the compound have been included as inset to facilitate comparison.

Ag^0 [32]. Fig. 2A also displays the evolution of the SOERS signal at 828 cm^{-1}, which can be denoted as voltaRamangram at 828 cm^{-1} [5] (orange line), where PAS shows a maximum before reducing the free Ag^+ ion, as is observed in Fig. 2A. As has been described in previous works [5,9], EC-SOERS is a surface-enhanced Raman scattering strategy which is observed at oxidation potentials on silver and copper electrodes in presence of a suitable precipitating agent. When a dielectric or semiconducting nanocrystal, AgCl nanocrystal in our case, is generated on the surface of the electrode, the bulk oxidation of the surface generates Ag^+ cations in the solution. These free cations mediate the enhancement of the Raman signal. SOERS can be defined as a Raman signal amplification mediated by metal cations, where a metal electrode-nanocrystal-metal cation-molecule interaction takes place [30]. As previously stated, the presence of all the components involved in the SOERS phenomenon, Ag^0–AgCl–Ag^+ and PAS in our case, yield a local field which amplifies the Raman signal as is illustrated at oxidation potentials, Fig. 2A. This behaviour is similar to AA and SA molecules at different Raman shifts as can be observed in Fig. S1.

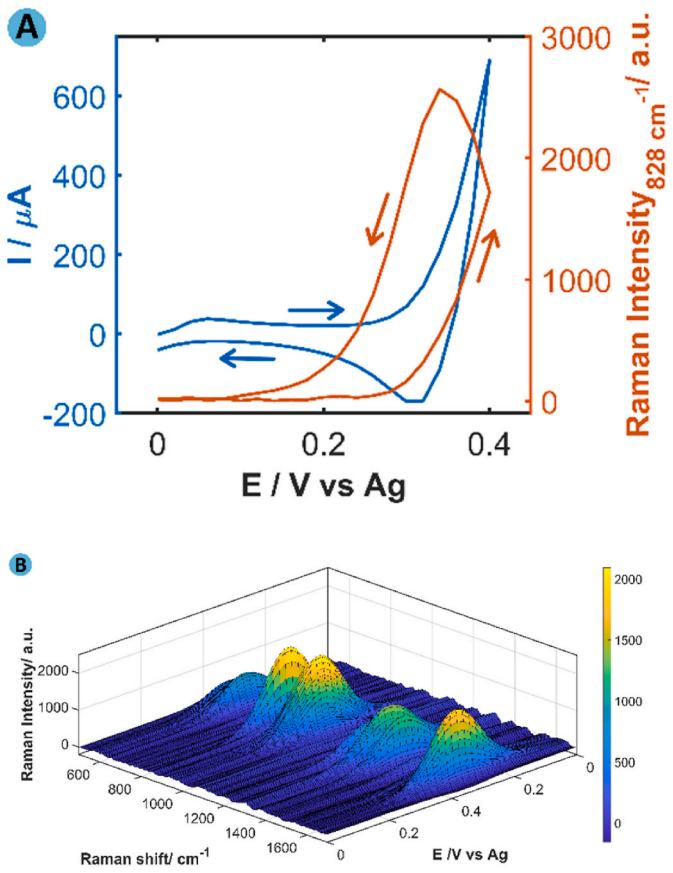

Fig. 2. (**A**) CV (blue line) and voltaRamangram (orange line) for a 25 μM PAS sample in 0.1 M $HClO_4$ and 5 mM KCl. The CV starts at 0 V in the anodic direction up to the vertex potentials (+0.40 V) at a scan rate of 0.02 Vs^{-1}. The voltaRamangram represents the evolution of the Raman intensity at 828 cm^{-1} versus the applied potential. (**B**) 3D plot of the evolution of the PAS Raman signal (between 450 and 1750 cm^{-1}) as a function of the applied potential. (For interpretation of the references to color in this figure legend, the reader is referred to the Web version of this article.)

Fig. 2B depicts a 3D plot, which illustrates how the Raman intensity varies in the fingerprint region between 450 and 1750 cm^{-1} as a function of the applied potential. As can be observed, the spectrum for PAS exhibits different bands which can be used to carry out the analytical study, namely, 828, 980 and 1627 cm^{-1}.

3.3. SPE performance

A novel type of SPEs have been developed for this study. These new SPEs were designed for best SEC analytical performance, reducing the fabrication costs. Considering that these SPEs are effectively single-use electrodes, because the WE surface becomes irreversibly modified during measurement, it was decided to print all three electrodes (WE, RE and CE) in silver. Using the same ink simplifies the fabrication process. After printing the three electrodes in the same step, the electrode areas are then defined by a printed dielectric coating, before dicing them out of the ceramic substrate.

After SPEs were manufactured, the electrodes were stored in vacuum bags in a non-oxidizing atmosphere, which contributes to their long-term preservation. Throughout the study, no significant changes in the stability of the SPE were observed, which indicates a good stability over time.

As Fig. S2A shows, both a commercial SPE with a graphite counter electrode (CE), and the new all-silver electrode SPE display the same electrochemical behaviour, which is essential for the generation of the Raman enhancement as mentioned above. Additionally, the spectroscopic information provided by these two different SPEs is very similar, with the Raman response being almost identical for the two SPEs, as shown in Fig. S2B.

In contrast to previous works [12,13,21], these novel SPEs fabricated with a different silver ink than the commercial ones, do not require pre-treatment prior to measurement. In fact, the new SPEs are roughened and the SOERS substrate is generated during the first experiment, allowing the simultaneous detection of the target molecule. Therefore, this new approach based on three electrodes of the same chemical composition can be successfully used to obtain well-defined Raman responses using a much more simplified three-electrode system.

3.4. Surface characterisation

SEM images of the Ag-SPE surface are shown in Fig. 3, being taken at different position. Fig. 3A and B were taken from an unmodified Ag-SPE whereas Fig. 3C and D were taken after a Raman-SEC experiment, stopping the voltammetry at +0.34 V potential in the cathodic scan in a 0.1 M $HClO_4$ and 5 mM KCl solution.

As Fig. 3A and B show, at the beginning of the experiment, the pristine surface of the Ag-SPE does not show any visible formation of nanostructures on the Ag surface. However, at a potential of +0.34 V in the backward scan of a TR-Raman-SEC experiment (Fig. 3C and D), numerous AgCl nanostructures were generated and homogeneously deposited on the WE Ag surface. These nanostructures are responsible for the Raman enhancement [32], with the maximum signal increase at this specific potential where the highest amount of Ag^+ is electrogenerated.

3.5. PAS determination using TR-Raman-SEC

To evaluate the linear correlation between the EC-SOERS signal and the PAS content, a range of concentrations between 2.5 and 20 μM were chosen, and a calibration model was prepared with five different standard samples which were replicated three times. The Raman signal at 828 cm^{-1} was selected as an example to represent voltaRamangrams at different concentrations (Fig. 4A) whereas +0.34 V in the cathodic direction was chosen as the optimum potential to obtain a higher sensitivity in the calibration (marked as dotted line in Fig. 4A). As Fig. 4B shows, three different calibration curves are represented at three selected Raman shifts, namely, 828, 980 and 1627 cm^{-1}, corresponding to the main EC-SOERS spectral peaks for PAS.

These three calibration curves showed a good linear correlation in the studied concentration range, resulting in the good analytical figures of merit given in Table 1. The limit of detection provides values better than the ones found in the literature [31,32], being our methodology more selective than measuring in the UV/Vis spectrum [31] and faster than performing a derivatization of the PA for obtaining a colored compound [32].

SERS substrates screening several orders of magnitude with logarithmic scale plot can be found in the literature, making it very difficult to discriminate between close concentration values. In our case, the ability of the methodology to discriminate very close analyte concentrations is highlighted by the fact that the study is performed in a much lower range with very good reproducibility of the SOERS responses.

After verifying the linearity of the method, a second calibration model with seven samples, each replicated three times, was carried out (see Table 2). In order to demonstrate the robustness of the method, the samples prepared for this calibration contain interferents from the same family of molecules (AA and SA), which have a very similar molecular structure and Raman spectra. Following the same procedure described previously, the Raman shift at +0.34 V in the cathodic direction was taken as an optimum point to assess the calibration model. The range of concentrations for PAS and interferents varies between 5 and 25 μM according to Table 2.

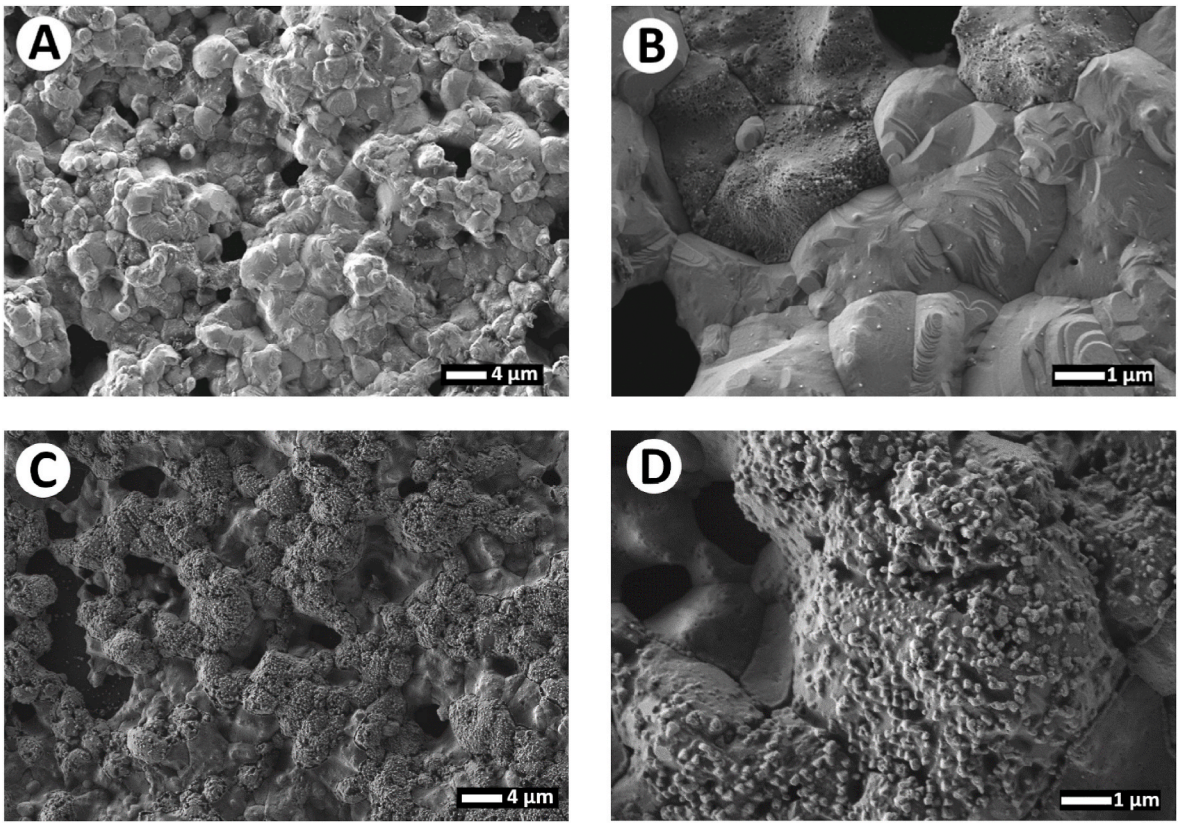

Fig. 3. SEM images of the Ag-SPEs surface during a SEC experiment. (**A, B**) Images of the Ag-SPE surface without any modification at different scale. (**C, D**) Images of the roughened Ag-SPE surface, taken at a potential of +0.34 (backward scan) at different scale.

Similar to the previous calibration model, three Raman shifts were taken from the spectra obtained by measuring these samples to represent the calibration curve, as shown in Fig. 5. It is noteworthy that the concentration of the three components are randomly selected, Table 2. Neither a fixed concentration of interfering compounds is added nor the three components are increased in a fixed amount between samples, which demonstrates the high capacity of the analytical methodology to analyze complex mixtures.

Good analytical figures of merit can be extracted from the calibration at the three Raman shifts, Table 3. When comparing Tables 1 and 3, we can observe a difference in their slopes, as well as in their LODs, which are higher for the calibration curves obtained in the presence of interferents. The performance of the calibration curves on different Ag-SPE batches would explain most of the differences in the slope. These problems, derived from the use of different Ag-SPE batches, will be solved when the electrode production is upscaled to industrial level, where large-scale manufacturing improves the reproducibility between numerous SPEs of the same batch.

As can be observed in Fig. S3, the samples containing 15 µM PAS, being MP3 and MP7 samples with interferents, and MP6, a sample which contains only PAS, show the same behavior, demonstrating than the presence of AA and SA, as interfering compounds, does not affect to the Raman response. SERS measurements showed a low dispersion, with RSDs below 10 % for all the measurements [2], Table S2. These results confirm that the different slopes between batches do not result from the presence of the interferents in the samples and also support the quality of the methodology.

The LODs values are in agreement with the expected values due to the presence of interferents. However, while in the simple calibration models (Table 1) the lowest LOD value corresponds to the curve represented at 828 cm^{-1}, in the case of calibration in presence of interferents (Table 3) the calibration model at 980 cm^{-1} exhibits the lowest value. This means that 980 cm^{-1} seems to be the more suitable Raman shift for determination of PAS in these experimental conditions.

To rationalize this result, the SOERS spectra of the three compounds was examined in detail. As Fig. S4A shows, the SOERS spectrum of the SA (yellow line) presents a high intensity band at 807 cm^{-1}. This band, close to 828 cm^{-1}, as well as the less intense bands corresponding to the AA spectrum centered at 807 and 847 cm^{-1} clearly interferes in the determination of PAS in these conditions. A similar behaviour is observed in the range 1500–1700 cm^{-1}, shown in Fig. S4B. However, the spectral interferences corresponding to AA and SA are minimal around 980 cm^{-1}, where we find a maximum for the PAS spectrum. In this regard, thanks to the nature of SEC techniques, we can move along the complete SOERS spectrum of PAS to select a specific Raman shift where the interfering behaviour of other compounds, in this case AA and SA, become minimal. Therefore, 980 cm^{-1} was chosen as the optimal Raman shift to determine PAS, obtaining very good results from the calibration curve.

To further evaluate the performance of the methodology, two commercial samples were chosen to determine the PAS content in a complex matrix, namely, Aspirin® and Adiro®. Both samples were prepared as specified in Section 2.5. The samples were measured in triplicate and the curve plotted at 980 cm^{-1} was used to predict the concentration of the test sample. Both samples contain a nominal concentration of 15 µM AA and a spiked concentration of 15 µM PAS, in addition to the excipients contained in the tablets of each drug. The regression curve predicts PAS concentrations of 14.6 and 14.1 µM for the Aspirin® and Adiro®, respectively, as shown in Table 4. Both results are remarkably close to the spiked concentration of PAS (15 µM), obtaining an accuracy of 97 ± 3 % and 94 ± 16 %, for the Aspirin® and Adiro®, respectively. From these results, we can state that the use of the new all silver SPEs, specifically optimized to work in SOERS, enables the determination of analytes in complex samples containing various interfering compounds.

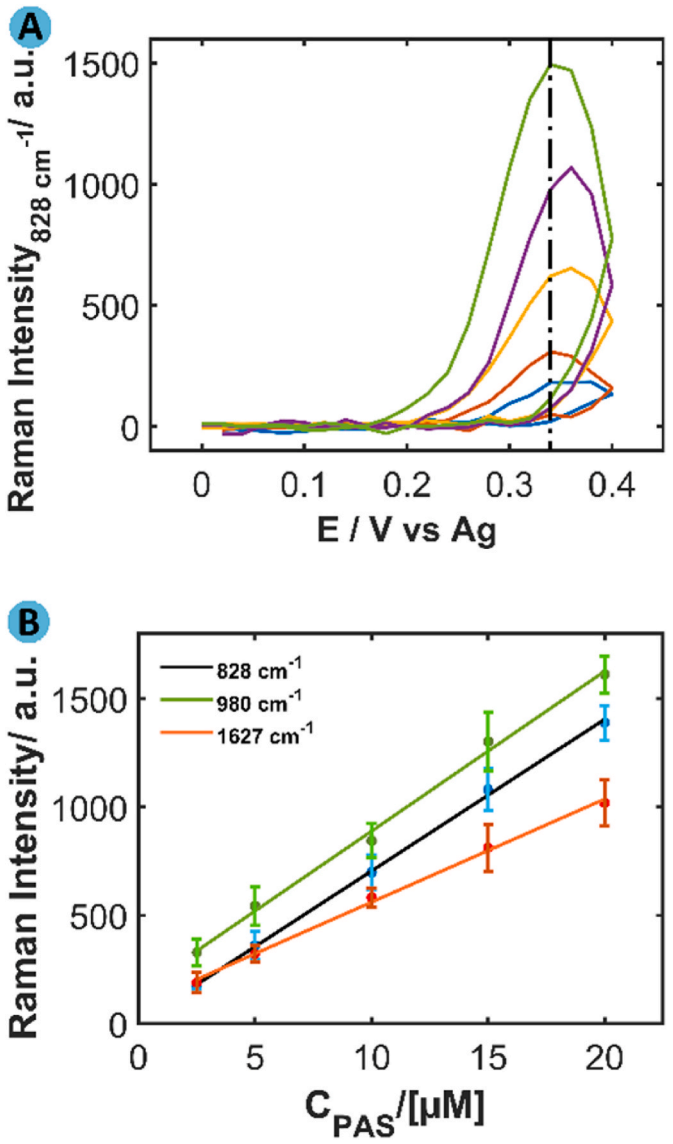

Fig. 4. (**A**) VoltaRamangrams at different concentrations of PAS [2.5, 5, 10, 15 and 20 μM] in presence of 0.1 M $HClO_4$ and 5 mM KCl, the signal at 828 cm^{-1} was selected for the illustration. The Raman intensity obtained at +0.34 V in the backward scan (dashed line) was chosen to construct the calibration models. (**B**) Calibration curve for PAS at +0.34 V in the backward scan for 828, 980 and 1627 cm^{-1}.

4. Conclusions

To the best of our knowledge, this is the first report of a novel three-electrode system for Raman spectroelectrochemistry, screen-printed using silver ink only. A comparative study with commercial SPEs used in previous works concludes that the performance of these novel SPEs is in line with that of commercial ones, yielding similar results both in electrochemistry and Raman spectroscopy, while reducing the manufacturing cost of the SPEs. Furthermore, the use of these brand-new SPEs in combination with TR-Raman-SEC has demonstrated to be an excellent analytical technique for the determination of PAS. The new TR-Raman-SEC method based on the oxidation/reduction of an Ag-SPE has been successfully used to determine PAS in Aspirin® and Adiro® samples, which contain potential interfering compounds. The results presented in this work demonstrate the robustness of this technique to carry out analytical determinations in complex samples, as well as the remarkable versatility of these new SPEs to be used in EC-SERS based analysis. These results can be potentially extended to other analytical problems, showing the high potential of the new combination shown herein. Further work needs to be done to demonstrate the analytical performance of the SEC sensor based on the SOERS for complex biological samples, such as, urine, blood serum or other body fluids.

CRediT authorship contribution statement

Luis Romay: Writing – review & editing, Writing – original draft, Visualization, Validation, Methodology, Investigation, Data curation, Conceptualization. **Pello Nuñez-Marinero:** Writing – review & editing, Supervision, Investigation, Formal analysis, Conceptualization. **Juan V.**

Table 2
Preparation of the calibration curve for PAS with AS and AA as interferents.

SAMPLE	[PAS]/μM	[AA]/μM	[SA]/μM
M1	5	25	0
M2	10	20	15
M3	15	0	25
M4	20	5	10
M5	25	15	20
M6	15	0	0
M7	15	15	15

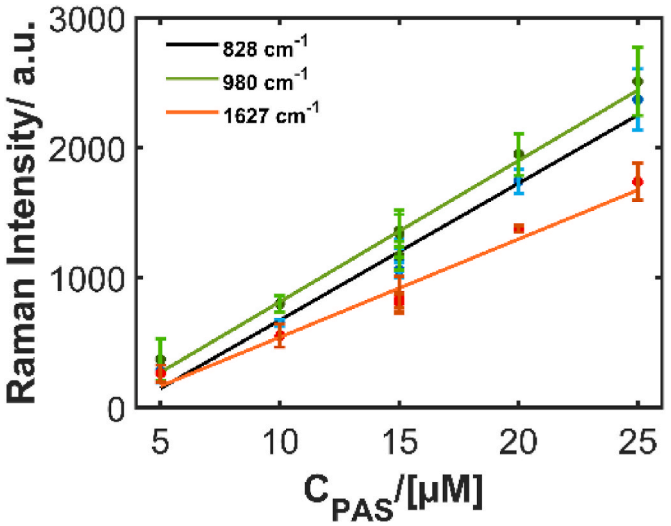

Fig. 5. Calibration curves for PAS in the presence of two interferents (AA and SA) at +0.34 V in the backward scan at three different Raman shift: 828, 980 and 1627 cm^{-1}.

Table 1
Analytical figures of merit for the linear regression models obtained at the Raman shift 828, 980 and 1627 cm^{-1} and +0.34 V in the backward scan during TR-Raman-SEC experiments.

Raman Shift (cm-1)	Slope (μM^{-1})	Slope Standard Error (μM^{-1})	Intercept (a.u.)	Intercept Standard Error (a.u)	R^2	S_{yx}	LOD (μM)
828	69.96	1.38	5.90	16.91	0.999	19.69	0.94
980	73.78	2.79	151.52	34.30	0.996	39.93	1.78
1627	47.61	1.38	85.29	16.96	0.997	19.73	1.36

R^2: Determination coefficient. S_{yx}: standard deviation of the calibration curve. LOD: limit of detection.

Table 3
Analytical figures of merit for the three linear regressions models obteined with samples from Table 2, with the Raman intensity values at 828, 980 and 1627 cm^{-1} at +0.34 V in the backward scan.

Raman Shift (cm^{-1})	Slope (μM^{-1})	Slope Standard Error (μM^{-1})	Intercept (a.u.)	Intercept Standard Error (a.u.)	R^2	S_{yx}	LOD (μM)
828	105.18	6.85	−377.86	110.56	0.979	108.27	3.39
980	107.99	6.34	−266.34	102.52	0.983	100.39	3.06
1627	75.43	5.90	−211.58	95.20	0.970	93.22	4.07

R^2: Determination coefficient. S_{yx}: standard deviation of the calibration curve. LOD: limit of detection.

Table 4
Prediction capability of PAS in complex test samples, using the calibration model constructed with Raman intensity at 980 cm^{-1} and at +0.34 V when running TR-Raman-SEC experiments, in presence of interferents (AA and SA).

Sample	Comercial Drug	$[C]_{spiked}$ (μM)	$[C]_{predicted}$ (μM)	Confidence Interval (μM)
TS_A	Aspirin® (BAYER)	15	14.6	14.2–15.0
TS_B	Adiro® (BAYER)	15	14.1	12.2–16.6

95,0 % confidence intervals for coefficient estimates.

Perales-Rondon: Writing – review & editing, Supervision, Investigation, Formal analysis, Conceptualization. **Aranzazu Heras:** Writing – review & editing, Resources, Project administration, Funding acquisition. **F. Javier del Campo:** Writing – review & editing, Writing – original draft, Validation, Supervision, Project administration, Methodology, Investigation, Funding acquisition, Formal analysis, Data curation, Conceptualization. **Alvaro Colina:** Writing – review & editing, Writing – original draft, Validation, Supervision, Project administration, Methodology, Investigation, Funding acquisition, Formal analysis, Data curation, Conceptualization.

Declaration of competing interest

The authors declare that they have no known competing financial interests or personal relationships that could have appeared to influence the work reported in this paper.

Data availability

Data will be available at the University of Burgos data repository

Acknowledgments

Ministerio de Ciencia e Innovación and Agencia Estatal de Investigación (MCIN/AEI/10.13039/501100011033, PID2020-113154RB-C21, PID2020-113154RB-C22), Junta de Castilla y León and European Regional Development Fund (Grant number: BU036P23), Ministerio de Ciencia, Innovación y Universidades (RED2022-134120-T) are gratefully acknowledged for funding this work. L.R. acknowledges Ministerio de Ciencia e Innovación and Agencia Estatal de Investigación (MCIN/AEI/10.13039/501100011033, PIS2020-113154 GB-C21) for the predoctoral contract. J.V. P.-R. acknowledges Ministerio de Universidades and NextGenerationEU for his Maria Zambrano fellowship.

Appendix. A Supplementary data

Supplementary data to this article can be found online at https://doi.org/10.1016/j.aca.2024.343095.

References

[1] M. Fleischmann, P.J. Hendra, A.J. McQuillan, Raman spectra of pyridine adsorbed at a silver electrode, Chem. Phys. Lett. 26 (1974) 163–166, https://doi.org/10.1016/0009-2614(74)85388-1.

[2] J. Langer, D. Jimenez de Aberasturi, J. Aizpurua, R.A. Alvarez-Puebla, B. Auguié, J. J. Baumberg, G.C. Bazan, S.E.J. Bell, A. Boisen, A.G. Brolo, J. Choo, D. Cialla-May, V. Deckert, L. Fabris, K. Faulds, F.J. García de Abajo, R. Goodacre, D. Graham, A. J. Haes, C.L. Haynes, C. Huck, T. Itoh, M. Käll, J. Kneipp, N.A. Kotov, H. Kuang, E. C. Le Ru, H.K. Lee, J.-F. Li, X.Y. Ling, S.A. Maier, T. Mayerhöfer, M. Moskovits, K. Murakoshi, J.-M. Nam, S. Nie, Y. Ozaki, I. Pastoriza-Santos, J. Perez-Juste, J. Popp, A. Pucci, S. Reich, B. Ren, G.C. Schatz, T. Shegai, S. Schlücker, L.-L. Tay, K. G. Thomas, Z.-Q. Tian, R.P. Van Duyne, T. Vo-Dinh, Y. Wang, K.A. Willets, C. Xu, H. Xu, Y. Xu, Y.S. Yamamoto, B. Zhao, L.M. Liz-Marzán, Present and future of surface-enhanced Raman scattering, ACS Nano 14 (2020) 28–117, https://doi.org/10.1021/acsnano.9b04224.

[3] R. Moldovan, E. Vereshchagina, K. Milenko, B.-C. Iacob, A.E. Bodoki, A. Falamas, N. Tosa, C.M. Muntean, C. Farcău, E. Bodoki, Review on combining surface-enhanced Raman spectroscopy and electrochemistry for analytical applications, Anal. Chim. Acta 1209 (2022) 339250, https://doi.org/10.1016/j.aca.2021.339250.

[4] S. Schlücker, Surface-enhanced Raman spectroscopy: concepts and chemical applications, Angew. Chem. Int. Ed. 53 (2014) 4756–4795, https://doi.org/10.1002/anie.201205748.

[5] C.L. Brosseau, A. Colina, J.V. Perales-Rondon, A.J. Wilson, P.B. Joshi, B. Ren, X. Wang, Electrochemical surface-enhanced Raman spectroscopy, Nat. Rev. Methods Prim. 3 (2023) 79, https://doi.org/10.1038/s43586-023-00263-6.

[6] I. Alessandri, J.R. Lombardi, Enhanced Raman scattering with dielectrics, Chem. Rev. 116 (2016) 14921–14981, https://doi.org/10.1021/acs.chemrev.6b00365.

[7] J.R. Lombardi, R.L. Birke, Theory of surface-enhanced Raman scattering in semiconductors, J. Phys. Chem. C 118 (2014) 11120–11130, https://doi.org/10.1021/jp5020675.

[8] X. Wang, W. Shi, S. Wang, H. Zhao, J. Lin, Z. Yang, M. Chen, L. Guo, Two-dimensional amorphous TiO 2 nanosheets enabling high-efficiency photoinduced charge transfer for excellent SERS activity, J. Am. Chem. Soc. 141 (2019) 5856–5862, https://doi.org/10.1021/jacs.9b00029.

[9] J.V. Perales-Rondon, S. Hernandez, D. Martin-Yerga, P. Fanjul-Bolado, A. Heras, A. Colina, Electrochemical surface oxidation enhanced Raman scattering, Electrochim. Acta 282 (2018) 377–383, https://doi.org/10.1016/j.electacta.2018.06.079.

[10] M. Perez-Estebanez, W. Cheuquepan, A. Heras, A. Colina, Electrochemically generated CuI and CuSCN nanocrystals on Cu surfaces as Raman enhancing substrates, Appl. Surf. Sci. 654 (2024) 159442, https://doi.org/10.1016/j.apsusc.2024.159442.

[11] S. Hernandez, W. Cheuquepan, M. Perez-Estebanez, A. Heras, A. Colina, Silver hexacyanoferrate (II) nanocrystals as a new material to improve Raman scattering enhancement during silver surface oxidation, Electrochim. Acta 465 (2023) 142994, https://doi.org/10.1016/j.electacta.2023.142994.

[12] M. Perez-Estebanez, W. Cheuquepan, M. Huidobro, J.V. Cuevas, S. Hernandez, A. Heras, A. Colina, Raman spectroelectrochemical determination of clopyralid in tap water, Microchem. J. 183 (2022) 108018, https://doi.org/10.1016/j.microc.2022.108018.

[13] S. Hernandez, J.V. Perales-Rondon, A. Heras, A. Colina, Enhancement factors in electrochemical surface oxidation enhanced Raman scattering, Electrochim. Acta 380 (2021) 138223, https://doi.org/10.1016/j.electacta.2021.138223.

[14] S. Hernandez, J.V. Perales-Rondon, A. Heras, A. Colina, Electrochemical SERS and SOERS in a single experiment: a new methodology for quantitative analysis, Electrochim. Acta 334 (2020) 135561, https://doi.org/10.1016/j.electacta.2019.135561.

[15] S. Hernandez, J.V. Perales-Rondon, A. Heras, A. Colina, Determination of uric acid in synthetic urine by using electrochemical surface oxidation enhanced Raman scattering, Anal. Chim. Acta 1085 (2019) 61–67, https://doi.org/10.1016/j.aca.2019.07.057.

[16] L. Vázquez-Iglesias, G.M. Stanfoca Casagrande, D. García-Lojo, L. Ferro Leal, T. A. Ngo, J. Pérez-Juste, R.M. Reis, K. Kant, I. Pastoriza-Santos, SERS sensing for cancer biomarker: approaches and directions, Bioact. Mater. 34 (2024) 248–268, https://doi.org/10.1016/j.bioactmat.2023.12.018.

[17] W. Cheuquepan, S. Hernandez, M. Perez-Estebanez, L. Romay, A. Heras, A. Colina, Electrochemical generation of surface enhanced Raman scattering substrates for the determination of folic acid, J. Electroanal. Chem. 896 (2021) 115288, https://doi.org/10.1016/j.jelechem.2021.115288.

[18] C. Hess, New advances in using Raman spectroscopy for the characterization of catalysts and catalytic reactions, Chem. Soc. Rev. 50 (2021) 3519–3564, https://doi.org/10.1039/D0CS01059F.

[19] C.L. Brosseau, F. Casadio, R.P. Van Duyne, Revealing the invisible: using surface-enhanced Raman spectroscopy to identify minute remnants of color in Winslow Homer's colorless skies, J. Raman Spectrosc. 42 (2011) 1305–1310, https://doi.org/10.1002/jrs.2877.

[20] T.P. Lynk, C.S. Sit, C.L. Brosseau, Electrochemical surface-enhanced Raman spectroscopy as a platform for bacterial detection and identification, Anal. Chem. 90 (2018) 12639–12646, https://doi.org/10.1021/acs.analchem.8b02806.
[21] D. Martín-Yerga, A. Pérez-Junquera, M.B. González-García, J.V. Perales-Rondon, A. Heras, A. Colina, D. Hernández-Santos, P. Fanjul-Bolado, Quantitative Raman spectroelectrochemistry using silver screen-printed electrodes, Electrochim. Acta 264 (2018) 183–190, https://doi.org/10.1016/j.electacta.2018.01.060.
[22] R. Moldovan, M. Perez-Estebanez, A. Heras, E. Bodoki, A. Colina, Activating the SERS features of screen-printed electrodes with thiocyanate for sensitive and robust EC-SERS analysis, Sens. Actuators, B 407 (2024) 135468, https://doi.org/10.1016/j.snb.2024.135468.
[23] S.A.B. Chotoye, M.M. Eisnor, R.B.E. Ball, C.L. Brosseau, Development of an electrochemical surface-enhanced Raman spectroscopic biosensor for the direct detection of glutathione, J. Raman Spectrosc. 54 (2023) 587–595, https://doi.org/10.1002/jrs.6522.
[24] R. Moldovan, K. Milenko, E. Vereshchagina, B.-C. Iacob, K. Schneider, C. Farcău, E. Bodoki, EC-SERS detection of thiabendazole in apple juice using activated screen-printed electrodes, Food Chem. 405 (2023) 134713, https://doi.org/10.1016/j.foodchem.2022.134713.
[25] S. Chakraborty, T. Gruber, C.E. Barry, H.I. Boshoff, K.Y. Rhee, Para -aminosalicylic acid acts as an alternative substrate of folate metabolism in, Mycobacterium tuberculosis, Science (80-) 339 (2013) 88–91, https://doi.org/10.1126/science.1228980.
[26] B.J. Wilson, B.W. Armstrong, Determination of para-aminosalicylic acid blood levels, Am. J. Clin. Pathol. 19 (1949) 886–890, https://doi.org/10.1093/ajcp/19.9_ts.886.
[27] E. Vasbinder, G. Van der Weken, Y. Vander Heyden, W.R.G. Baeyens, A. Debunne, J.P. Remon, A.M. García-Campaña, Quantitative determination of p -aminosalicylic acid and its degradation product m -aminophenol in pellets by ion-pair high-performance liquid chromatography applying the monolithic Chromolith Speedrod RP-18e column, Biomed. Chromatogr. 18 (2004) 55–63, https://doi.org/10.1002/bmc.292.
[28] L. Hong, W. Jiang, W. Zheng, S. Zeng, HPLC analysis of para-aminosalicylic acid and its metabolite in plasma, cerebrospinal fluid and brain tissues, J. Pharm. Biomed. Anal. 54 (2011) 1101–1109, https://doi.org/10.1016/j.jpba.2010.11.031.
[29] C.Y. Panicker, H.T. Varghese, A. John, D. Philip, K. Istvan, G. Keresztury, FT-IR, FT-Raman and FT-SERS spectra of 4-aminosalicylic acid sodium salt dihydrate, Spectrochim. Acta Part A Mol. Biomol. Spectrosc. 58 (2002) 281–287, https://doi.org/10.1016/S1386-1425(01)00541-8.
[30] S. Hernandez, M. Perez-Estebanez, W. Cheuquepan, J.V. Perales-Rondon, A. Heras, A. Colina, Raman, UV–vis absorption, and fluorescence spectroelectrochemistry for studying the enhancement of the Raman scattering using nanocrystals activated by metal cations, Anal. Chem. 95 (2023) 16070–16078, https://doi.org/10.1021/acs.analchem.3c01172.
[31] C. Vetuschi, G. Ragno, P. Mazzeo, Determination of p-aminosalicylic acid and m-aminophenol by derivative UV-spectrophotometry, J. Pharm. Biomed. Anal. 6 (1988) 383–391, https://doi.org/10.1016/0731-7085(88)80003-7.
[32] M. Laghari, Y. Darwis, A. Memon, New spectrophotometric methods for the determination of p-aminosalicylic acid in tablets, Trop. J. Pharmaceut. Res. 13 (2014) 1133, https://doi.org/10.4314/tjpr.v13i7.18.